Neurobiology of Disease 43 (2011) 715–724

Contents lists available at ScienceDirect

Neurobiology of Disease

journal homepage: www.elsevier.com/locate/ynbdi

Familial Parkinson disease mutations influence α-synuclein assembly

Kenjiro Ono, Tokuhei Ikeda, Jun-ichi Takasaki, Masahito Yamada *

Department of Neurology and Neurobiology and Aging, Kanazawa University Graduate School of Medical Science, Kanazawa, Japan

ARTICLE INFO

Article history:
Received 18 March 2011
Revised 16 May 2011
Accepted 31 May 2011
Available online 7 June 2011

Keywords:
Parkinson's disease
α-Synuclein
Mutations
Oligomers
Electron microscopy
Atomic force microscopy

ABSTRACT

Lewy bodies composed of aggregates of α-synuclein (αS) in the brain are the main histopathological features of Lewy body diseases (LBD) such as Parkinson's disease and dementia with Lewy bodies. Mutations such as E46K, A30P and A53T in the αS gene cause autosomal dominant LBD in a number of kindreds. Although these mutations accelerate fibril formation, their precise effects at early stages of the αS aggregation process remain unknown. To answer this question, we examined the aggregation including monomer conformational dynamics and oligomerization of the E46K, A30P, A53T and A30P/A53T mutations and wild type (WT) using thioflavin S assay, circular dichroism spectroscopy, photo-induced cross-linking of unmodified proteins, electron microscopy, and atomic force microscopy. Relative to WT αS, E46K αS accelerated the kinetics of the secondary structure change and oligomerization, whereas A30P αS decelerated them. These effects were reflected in changes in average oligomer size. The mutant oligomers of E46K αS functioned as fibril seeds significantly more efficiently than those of WT αS, whereas the mutant oligomers of A30P αS were less efficient. Our results that mutations of familial LBD had opposite effects at early stages of αS assembly may provide new insight into the molecular mechanisms of LBD.

Introduction

Parkinson's disease (PD) is a neurodegenerative movement disorder characterized by the selective loss of dopaminergic neurons from the substantial nigra, and the appearance of intraneuronal inclusions, called Lewy bodies (LBs) and Lewy neurites. LBs are composed of a dense core of fibrillar structures whose major component is α-synuclein (αS) (Baba et al., 1998; Spillantini et al., 1998). Aggregation of αS is considered to be an important and, probably, seminal step in the development of Lewy body diseases (LBD) including PD and dementia with LBs (DLB) and other α-synucleinopathies such as multiple system atrophy (Ono et al., 2008; Uversky, 2007).

Genetic studies of the αS gene in familial cases of PD and DLB have demonstrated that expression of abnormal αS or overexpression of normal αS is associated with these diseases. Pathogenic missense mutations [A53T (Polymeropoulos et al., 1997), A30P (Kruger et al., 1998), and E46K (Zarranz et al., 2004) and multiplication (Chartier-Harlin et al., 2004; Farrer et al., 2004; Fuchs et al., 2007; Ibanez et al., 2004; Nishioka et al., 2006; Singleton et al., 2003)] of the αS gene have been identified in kindreds of autosomal dominantly inherited familial PD and DLB (Fig. 1).

αS is a 140-amino acid protein, having an N-terminal domain with seven imperfect KTKEGV sequence repeats, followed by a hydrophobic central region (non-amyloid β-protein (Aβ) component of Alzheimer disease (NAC)) and C-terminal domain with a large portion of acidic residues. The repeat region at the N-terminus has been assumed to form an amphipathic α-helix by binding to phospholipid (Davidson et al., 1998). Circular dichroism and Fourier-transform IR analysis revealed that αS is a natively unfolded protein without a highly ordered secondary structure (Uversky et al., 2001). Recent nuclear magnetic resonance (NMR) analyses have revealed three intramolecular long range interactions. These interactions are between the highly hydrophobic NAC region (residues 85–95) and the C terminus (residues 110–130), C-terminal residues 120–130 and residues 105–115, and the region around residue 120 and the N terminus around residue 20 (Bertoncini et al., 2005b; Bussell and Eliezer, 2001; Dedmon et al., 2005).

Upon incubation at 37 °C at a high concentration with agitation, recombinant αS assembles into fibrils that closely resemble those in the PD or DLB brain (Conway et al., 1998, 2000a). Assembly of αS into αS fibrils (fαS) follows a nucleation-dependent process that consists of a lag phase (nucleation) and a growth phase (elongation) (Wood et al., 1999). The prevalence of fαS associated with LBD has led many researchers to hypothesize that they cause cell death (Duda et al., 2000; Spillantini et al., 1998). However, recent evidence suggests that the earlier intermediates, αS oligomers may be more toxic components (Danzer et al., 2007; Karpinar et al., 2009; Outeiro et al., 2008; Wright et al., 2009).

αS, which is predominantly non-phosphorylated in vivo under normal conditions (Fujiwara et al., 2002), is extensively phosphorylated at Ser129 in α-synucleinopathic lesions (Fujiwara et al., 2002; Nishie et al., 2004). The specific phosphorylation of αS at Ser129 by

* Correspondence author. Fax: +81 76 234 4253.
E-mail address: m-yamada@med.kanazawa-u.ac.jp (M. Yamada).
Available online on ScienceDirect (www.sciencedirect.com).

0969-9961/$ – see front matter © 2011 Elsevier Inc. All rights reserved.
doi:10.1016/j.nbd.2011.05.025

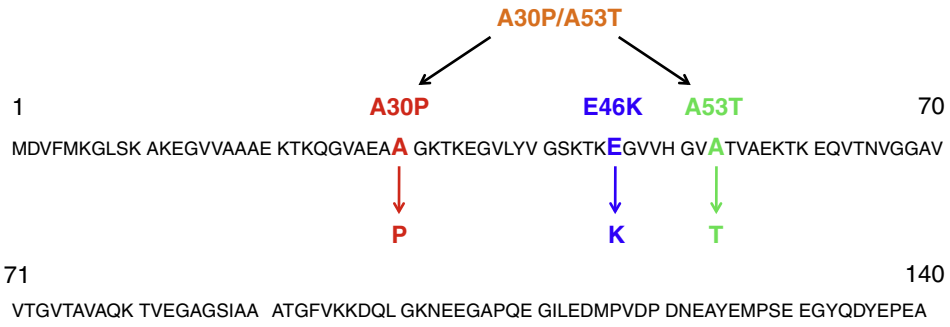

Fig. 1. Amino acid sequences of αS.

casein kinase 2 (Okochi et al., 2000; Pronin et al., 2000) resulted in accelerated oligomerization and formation of fαS (Fujiwara et al., 2002).

Mutations such as E46K, A30P and A53T have been reported to influence fαS formation in vitro (Conway et al., 1998, 2000b; Fredenburg et al., 2007; Giasson et al., 1999; Goldberg and Lansbury, 2000; Greenbaum et al., 2005; Narhi et al., 1999; Yonetani et al., 2009). The A53T mutation increased the propensity of fαS formation as well as the formation of protofibrils (Conway et al., 1998, 2000b; Giasson et al., 1999; Narhi et al., 1999). The A30P mutation promoted the formation of protofibrils but not that of fαS (Conway et al., 2000b; Goldberg and Lansbury, 2000) and some of the protofibrils with a circular morphology formed pores by binding to the ER membrane (Volles and Lansbury, 2002). The E46K mutation has also been reported to increase the propensity of fαS formation (Greenbaum et al., 2005), and reduce the propensity of protofibrils by lower permeability of lipid vesicles (Fredenburg et al., 2007).

Here, we focused on the earliest stages of αS aggregation including monomer conformational dynamics and formation of low order oligomers of wild type (WT), E46K, A30P, A53T and A30P/A53T αS. Our results showed that the E46K mutation produces αS peptides displaying accelerated statistical coil→α/β→β secondary structure transitions and an increased propensity to form relatively large oligomers, whereas the A30P mutation produces αS peptides displaying decelerated secondary structure transitions and a decreased propensity to form oligomers. These results that familial mutations have reverse effects on early stages of αS assembly may be useful for understanding the pathological mechanism of LBD.

Materials and methods

Chemicals and reagents

Chemicals were obtained from Sigma-Aldrich Co. (St. Louis, MO) or Invitrogen (Carlsbad, CA) and were of the highest purity available. Water was produced using a Milli-Q system (Millipore Corp., Bedford, MA).

Peptides

The αS solutions were prepared as described previously (Ono and Yamada, 2006). Briefly, wild-type αS (WT) (lot number 50306AS), E46K mutant αS (E46K) (lot number 90204ASK), A30P mutant αS (A30P) (lot number 10604ASP), A53T mutant αS (A53T) (lot number 61803AST), and A30P/A53T mutant αS (A30P/A53T) (lot number 30104ASPT) (Fig. 1) were purchased from Recombinant Peptide Technologies (LLC, GA, USA) and were stored at −80 °C.

αS peptides were dissolved at a nominal concentration of 70 μM in 20 mM Tris buffer, pH 7.4. After sonication for 1 min in a bath sonicator, the αS solution was centrifuged for 15 min at 16,000×*g*. We confirmed that pH of all samples were ≈7.6.

Peptide aggregation

Each αS solution prepared above (0.6 ml aliquot) was placed in a 1 ml microcentrifuge tube. The tubes were incubated at 37 °C for 0–7 d with agitation. Note that for each sample at each time point analyzed, aliquots used for different experiments (see below) were taken from the same tube of αS, ensuring that valid correlations could be made for the data thus produced.

Thioflavin S (ThS) binding

ThS solution contained 5 μM ThS (MP Biomedicals, LLC, Irvine, CA) and 50 mM of glycine–NaOH buffer, pH 8.5. 5-μl of each sample was added to 1 ml ThS solution, and then the mixture was vortexed briefly (≈3 s). Fluorescence was determined three times at intervals of 10 s using a Hitachi F-2500 fluorometer. Excitation and emission wavelengths were 440 and 521 nm, respectively. Fluorescence was determined by averaging the three readings and subtracting the fluorescence of a ThS blank.

Circular dichroism spectroscopy (CD)

CD measurements were made by placing 200 μl of sample into a 1 mm path-length CD cuvette (World Precision Instruments, Sarasota, FL), and acquiring spectra in a J-805 spectropolarimeter (JASCO, Tokyo, Japan). The CD cuvettes were maintained on ice prior to introduction into the spectrometer. Following temperature equilibration (≈20 min), spectra were recorded at 22 °C in the range of ≈190–260 nm at 0.2 nm resolution with a scan rate of 100 nm/min. Ten scans were acquired and averaged for each sample. Raw data were manipulated by smoothing and subtraction of buffer spectra according to the manufacturer's instructions. The half-time ($t_{1/2}$) for assembly-dependent conformational change was determined numerically from the formula $([\theta]_t - [\theta]_{min})/([\theta]_{max} - [\theta]_{min}) = 1/2$; where molar ellipticity $[\theta]$ always is measured at 198 nm, $[\theta]_t$ is molar ellipticity at time t, $[\theta]_{max}$ is maximal ellipticity, and $[\theta]_{min}$ is minimum ellipticity.

Photo-induced cross-linking of unmodified proteins (PICUP) and sodium dodecyl sulfate-polyacrylamide gel electrophoresis (SDS-PAGE)

Cross-linking of αS was photo-induced essentially as described (Bitan et al., 2001). Briefly, for αS, the general method was to mix 18 μl of peptide, at a nominal concentration of 70 μM, with 1 μl of 40 mM tris(2,2′-bipyridyl)dichlororuthenium(II) hexahydrate (Ru(bpy)) and 1 μl of 2 mM ammonium persulfate, both dissolved in 20 mM Tris buffer, pH 7.4. Then the mixtures were irradiated for 1 s with visible light and the reaction was quenched with 1 μl of 1 M dithiothreitol (Invitrogen) in water. The frequency distribution of monomers and oligomers was determined using SDS-PAGE and silver staining, as described (Bitan et al., 2001). Briefly, 20 μl of each cross-

linked sample was electrophoresed on a 10–20% gradient tricine gel and visualized by silver staining (SilverXpress, Invitrogen). Non-cross-linked samples were used as controls in each experiment. Densitometry was then performed using a luminescent image analyzer (LAS 4000 mini, Fujifilm, Tokyo) and image analysis software (Multi gauge version 3.2, Fujifilm).

Nucleation activity of cross-linked αS oligomers

αS peptides were dissolved in 20 mM Tris buffer, pH 7.4, to produce final concentrations of 70 μM. After sonication for 1 min using a bath sonicator, the peptide solutions were centrifuged for 15 min at 16,000×*g*. fαS or cross-linked αS, of the E46K, A30P, A53T and A30P/A53T analogs, were also prepared at a concentration of 70 μM in 20 mM Tris buffer, pH 7.4. The sonicated fαS or cross-linked αS were added to the un-cross-linked peptides at a ratio of 10% (v/v). The mixtures were incubated at 37 °C for 0–7 d without agitation.

Electron microscopy (EM)

A 10 μl aliquot of each sample was spotted onto a glow-discharged, carbon-coated Formvar grid (Okenshoji Co. Ltd, Tokyo, Japan) and incubated for 20 min. The droplet was displaced with an equal volume of 2.5% (v/v) glutaraldehyde in water and incubated for an additional 5 min. Finally, the peptide was stained with 8 μl of 1% (v/v) filtered (0.2 μm) uranyl acetate in water (Wako Pure Chemical Industries Ltd, Osaka, Japan). This solution was wicked off and then the grid was air-dried. Samples were examined using a JEM-1210 transmission electron microscope. The diameters of assemblies were measured using a 10× magnifier eyepiece containing a graticule (Electron Microscopy Sciences).

Atomic force microscopy (AFM)

Peptide solutions were characterized using a Nanoscope IIIa controller (Veeco Digital Instruments, Santa Barbara, CA) with a multimode scanning probe microscope equipped with a JV scanner. All measurements were carried out in the tapping mode under ambient conditions using single-beam silicon cantilever probes. A 10 μl aliquot of each sample was spotted onto freshly cleaved mica (Ted Pella, Inc., Redding, CA), incubated at room temperature for 5 min, rinsed with water, and then blown dry with air. At least four regions of the mica surface were examined to confirm the homogeneity of the structures throughout the sample. Mean particle heights were analyzed by averaging the measured values of eight individual cross-sectional line scans from each image only when the particle structure was confirmed.

Results

Assemblies of WT and mutant[1] αS peptides

To determine the effects of E46K, A30P, A53T and A30P/A53T substitutions on αS assembly, we used a well characterized assay of fibril formation, thioflavin dye binding (LeVine, 1993, 1999; Naiki and Nakakuki, 1996). We found that E46K, A53T and A30P/A53T αS peptides accelerated fαS formation compared with the WT αS peptide (Fig. 2). On the other hand, A30P αS peptide decelerated fibril formation compared with WT αS peptide (Fig. 2). To further determine the effects of E46K, A30P, A53T and A30P/A53T mutations on the details of fαS formation such as nucleation and elongation phases, we analyzed the lag time, growth rate and maximum intensity (Table 1). Although the lag time meaning nucleation phase mainly was similar in WT and all mutant αS peptides, E46K, A53T and A30P/A53T αS peptides increased the growth rate meaning elongation phase compared with the WT αS peptide (Table 1). On the other hand, the A30P peptide decreased the growth rate compared with the WT αS peptide (Table 1). The overall activity of fαS formation was in the order of: E46K>A53T=A30P/A53T>WT>A30P.

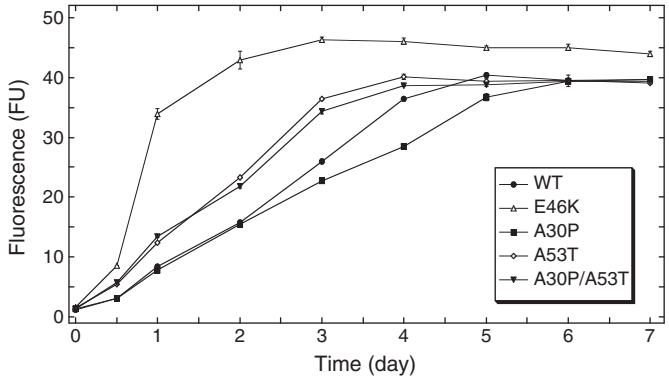

Fig. 2. ThS binding. 70 μM αS of WT (○), E46K (△), A30P (■), A53T (◇) or A30P/A53T (▼) was incubated at 37 °C for 7 days in 20 mM Tris buffer, pH 7.4. Periodically, aliquots were removed and ThS binding levels were determined. Binding is expressed as mean fluorescence (in arbitrary fluorescence units (FU)) ± S.E. Each figure comprises data obtained with 3 independent experiments.

We used EM to directly confirm the fαS formation of WT, E46K, A30P, A53T and A30P/A53T after incubation at 37 °C for 7 d. WT and all mutant αS fibrils formed a uniformly long, non-branched filament structure and there were no clear differences morphologically (Fig. 3). The diameters of WT (Fig. 3A), E46K (Fig. 3B), A30P (Fig. 3C), A53T (Fig. 3D) and A30P/A53T (Fig. 3E) fαS were 10.8 ± 0.4, 10.3 ± 0.5, 9.3 ± 0.4, 10.9 ± 0.4 and 9.6 ± 0.9 (mean ± S.E., n = 10) nm, respectively.

Secondary structure dynamics of wild type and mutant αS peptides

To analyze the secondary structure dynamics of WT αS isoforms and mutants thereof, we monitored peptide folding and assembly systems by CD during 7 d of incubation at 37 °C. All five peptides initially produced spectra consistent with primarily statistical coil (SC) secondary structure (Figs. 4A–E). The major feature of these spectra was a large magnitude minimum centered at ≈198 nm. To allow comparison of the kinetics among the five peptides, the half-time ($t_{1/2}$) for the entire transition process was determined using $[\theta]_{198}$, which correlates with SC, as a metric (see Methods).

WT αS displayed substantial secondary structure changes during days 1–6 that were consistent with SC → α/β → β transitions associated with monomer → protofibril → fibril assembly (Fig. 4A).

Table 1
Kinetics of αS assembly.

Sample	Lag time (d)[a]	Growth rate (FU/d)[b]	Maximum intensity (FU)[c]
WT αS	0.5	10.4	40.4
E46K αS	0.3	25.4	44.9
A30P αS	0.5	8.2	39.6
A53T αS	0.3	13.1	39.5
A30P/A53T αS	0.3	12.5	39.4

[a] Lag time was defined as the point of intersection with the abscissa of the line determined by the pseudo-linear portion of the fluorescence progress curve, according to Evans *et al.* (Evans et al., 1995).
[b] Growth rate was determined by line fitting to the pseudo-linear segment of the ascending portion of the fluorescence progress curve.
[c] Determined by visual inspection.

[1] We refer to the E46K, A30P, A53T and A30P/A53T peptides as "mutants" only for ease in distinguishing them from WT αS. This designation does not refer directly to the corresponding DNA sequences.

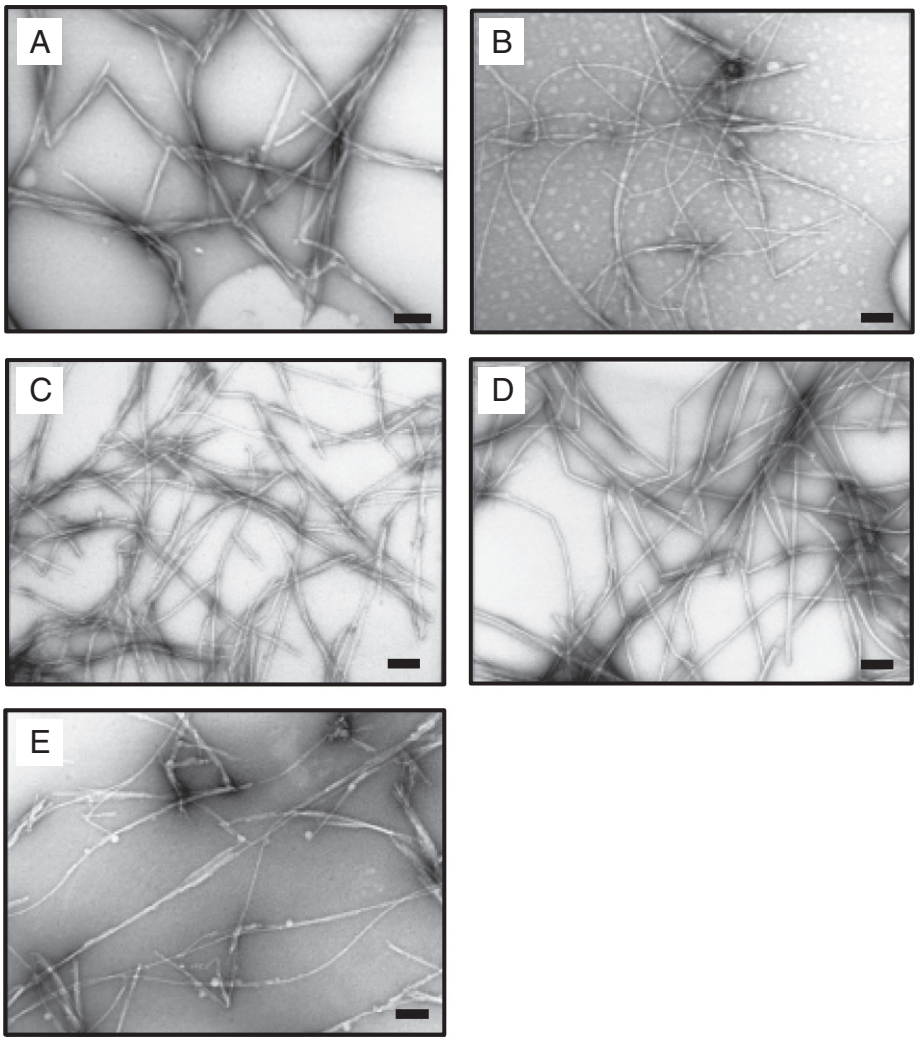

Fig. 3. αS assembly morphology. EM was used to determine the morphologies of assemblies of αS. 70 μM αS of WT (A), E46K (B), A30P (C), A53T (D) or A30P/A53T (E) was incubated at 37 °C for 7 days in 20 mM Tris buffer, pH 7.4. Scale bars indicate 100 nm.

For WT αS, $t_{1/2}$ was ≈1.5 d (Fig. 4F). E46K αS displayed substantially accelerated kinetic, with $t_{1/2}$≈0.6 d (Figs. 4B and F). Conformational change in E46K αS was complete by day 2. A30P αS displayed substantial secondary structure changes during days 1–6, with $t_{1/2}$≈1.6 d (Figs. 4C and F). The A53T and A30P/A53T αS peptides displayed slightly accelerated kinetics, with $t_{1/2}$≈1.1 d (Figs. 4D, E and F). Conformational changes in the A53T and A30P/A53T αS peptides were complete by day 5 and the spectra during days 1–5 were very similar. The maximal value of $d[\theta]/dt$ of E46K αS was strikingly high, but similar for the other three mutant and WT αS peptides (Fig. 4F).

αS oligomerization

To determine whether the E46K, A30P, A53T or A30P/A53T amino acid substitutions affected peptide oligomerization, we used PICUP, a photochemical cross-linking method that is rapid, efficient, requires no structural modification of peptides, and accurately reveals the oligomerization state of peptides (for a review, see Bitan and Teplow, 2004). In the un-cross-linked controls, the WT αS peptide was composed primarily of monomers (Fig. 5, lane 1). Similar patterns were observed for the homologous E46K, A30P, A53T or A30P/A53T αS peptides (Fig. 5, lanes 2–5). When the oligomers were stabilized by cross-linking, WT αS was composed of monomers to tetramers (Fig. 5, lane 6), whereas E46K αS was composed of higher order species, including pentamers and hexamers (Fig. 5, lane 7). The oligomers of A30P αS were composed of monomers to trimers (Fig. 5, lane 8). The oligomers of both A53T and A30P/A53T αS peptides showed a distribution similar to that of WT αS (Fig. 5, lanes 9 and 10). The oligomer/monomer ratios of WT, E46K, A30P, A53T and A30P/A53T αS peptides are 1.64 ± 0.12, 1.98 ± 0.07, 0.73 ± 0.02. 1.63 ± 0.12, and 1.68 ± 0.12, respectively (n = 3, mean ± S.E.). We note that a new band appeared below the band corresponding to the monomer, which might be truncated αS by autocatalytic proteolysis.

αS assembly morphology

We examined the morphology of the oligomers formed immediately following peptide dissolution by EM (Fig. 6; Table 2) and AFM (Fig. 7; Table 2). Un-cross-linked αS of WT and all mutant αS peptides showed an irregular globular structure (Fig. 6). The average diameter of the globular components was 2.17 ± 0.13 (mean ± S.E.) nm (Fig. 6A and Table 2). Although un-cross-linked mutant αS peptides produced a similar globular structure, the average diameters of E46K (Fig. 6B), A30P (Fig. 6C), A53T (Fig. 6D) and A30P/A53T (Fig. 6E) un-cross-linked αS were 2.95 ± 0.34, 1.95 ± 0.30, 2.16 ± 0.19 and 2.16 ± 0.42 (mean ± S.E.) nm, respectively (Table 2).

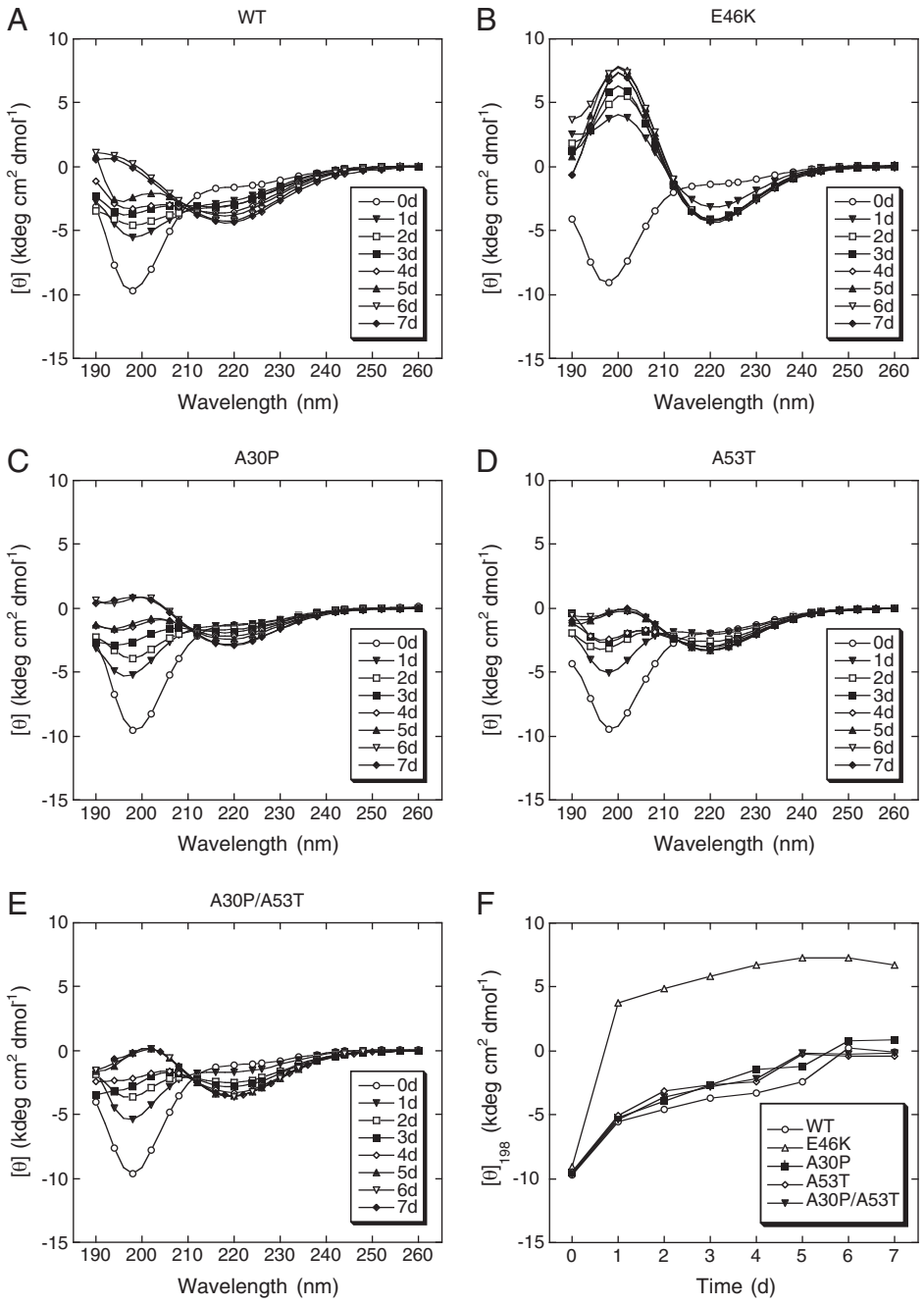

Fig. 4. αS secondary structure dynamics. 70 μM αS of WT (A), E46K (B), A30P (C), A53T (D) or A30P/A53T (E) was incubated at 37 °C for 7 days in 20 mM Tris buffer, pH 7.4. Spectra were acquired immediately at the start of the incubation period, d 0 (○), and after days 1 (▼), 2 (□), 3 (■), 4 (◇), 5 (▲), 6 (▽) and 7 (♦). The spectra presented at each time are representative of those obtained during each of 3 independent experiments. (F) Molar ellipticity $[\ ]_{198}$ versus time for αS.

The cross-linked oligomers of WT αS peptide were predominantly quasi-spherical or ellipsoidal globular with an average diameter of 10.85 ± 1.05 (mean ± S.E.) nm (Fig. 6F; Table 2). The cross-linked oligomers of A53T and A30P/A53T αS peptides had a similar morphology with diameters of 10.79 ± 0.82 and 10.98 ± 0.97 nm, respectively (Figs. 6I and J; Table 2). Cross-linked oligomers of E46K αS had the largest globules with an average diameter of 14.97 ± 1.81 nm (Fig. 6G; Table 2). Relative to WT αS, E46K, A53T or A30P/A53T αS, cross-linked oligomers of A30P αS had smaller globules with an average diameter of 9.99 ± 0.58 nm (Fig. 6H; Table 2).

AFM studies showed similar results. The average height of the globular components was 0.50 ± 0.01 (mean ± S.E.) nm (Fig. 7A and Table 2). Although un-cross-linked mutant αS peptides produced a similar globular structure, the average height of E46K (Fig. 7B), A30P (Fig. 7C), A53T (Fig. 7D) and A30P/A53T (Fig. 7E) un-cross-linked αS was 0.65 ± 0.02, 0.36 ± 0.01, 0.46 ± 0.01 and 0.44 ± 0.01 (mean ± S.E.) nm, respectively (Table 2).

The average height of cross-linked oligomers of WT αS peptide was 1.51 ± 0.12 (mean ± S.E.) nm (Fig. 7F; Table 2). The cross-linked oligomers of A53T and A30P/A53T αS peptides had a similar morphology with a height of 1.46 ± 0.21 and 1.62 ± 0.15 nm, respectively (Figs. 7I and J; Table 2). Cross-linked oligomers of E46K αS had the largest globules with an average height of 3.36 ± 0.44 nm (Fig. 7G; Table 2). Relative to WT αS, E46K, A53T or A30P/A53T αS, cross-linked oligomers of A30P αS had smaller globules with an average height of 1.16 ± 0.17 nm (Fig. 7H; Table 2).

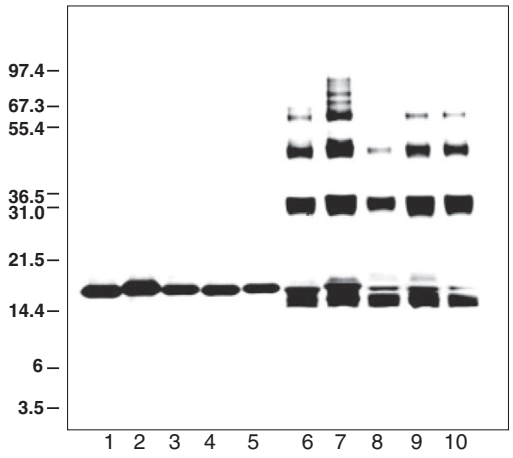

Fig. 5. αS oligomerization. PICUP, followed by SDS-PAGE and silver staining, was used to study oligomerization of 70 μM αS of WT, E46K, A30P, A53T or A30P/A53T. Lane 1, un-cross-linked αS of WT; lane 2, un-cross-linked αS of E46K; lane 3, un-cross-linked αS of A30P; lane 4, un-cross-linked αS of A53T; lane 5, un-cross-linked αS of A30P/A53T; lane 6, cross-linked αS of WT; lane 7, cross-linked αS of E46K; lane 8, cross-linked αS of A30P; lane 9, cross-linked αS of A53T; lane 10, cross-linked αS of A30P/A53T. The gel is representative of three independent experiments.

Table 2
Morphological analysis of αS assemblies[a].

Assembly	Diameter [a]	Height [b]
Un-cross-linked WT	2.17 ± 0.13 (19)	0.50 ± 0.01 (113)
Un-cross-linked E46K	2.95 ± 0.34 (23)	0.65 ± 0.02 (95)
Un-cross-linked A30P	1.95 ± 0.30 (19)	0.36 ± 0.01 (138)
Un-cross-linked A53T	2.16 ± 0.19 (25)	0.46 ± 0.01 (89)
Un-cross-linked A30P/A53T	2.16 ± 0.42 (26)	0.44 ± 0.01 (88)
Cross-linked WT	10.85 ± 1.05 (16)	1.51 ± 0.12 (40)
Cross-linked E46K	14.97 ± 1.81 (19)	3.36 ± 0.44 (23)
Cross-linked A30P	9.99 ± 0.58 (19)	1.16 ± 0.17 (20)
Cross-linked A53T	10.79 ± 0.82 (23)	1.46 ± 0.21 (27)
Cross-linked A30P/A53T	10.98 ± 0.97 (14)	1.62 ± 0.15 (37)

[a] Mean diameter ± S.E., in nm, is listed for (*n*) αS assemblies visualized by EM.
[b] Mean height ± S.E., in nm, is listed for (*n*) αS assemblies visualized by AFM.

Nucleation of αS fibril assembly

αS assembly has characteristics of a nucleation-dependent polymerization process (Wood et al., 1999). To study the abilities of fαS or oligomers of the WT and mutant αS peptides to nucleate fibril formation, we monitored the time-dependence of ThS fluorescence in seeded fibril formation experiments (Figs. 8 and 9). Thioflavin dye fluorescence does not measure fibril concentration per se (some fibrils do not possess the β-sheet structures to which Thioflavin dye binds) (Groenning, 2009), but the fluorescence intensity is correlated with fibril content (LeVine, 1993, 1999; Naiki and Nakakuki, 1996).

Un-seeded αS of WT displayed a quasi-sigmoidal process curve characterized by an ≈12 h lag time, an ≈108 h period of increasing ThS binding, and a binding plateau occurring after ≈120 h (Fig. 2)—results consistent with a nucleation-dependent polymerization process. The unseeded reaction displayed no initial fluorescence increase (Fig. 2). First, we examined nucleation activities of sonicated fαS. Adding 10% (w/w) sonicated fαS of WT eliminated the lag period and produced a quasi-hyperbolic increase in fluorescence that reached maximal levels at ≈6 h (Fig. 8A). Nucleation activity was displayed by other mutant fαS of E46K, A30P, A53T and A30P/A53T as well (Fig. 8A). To compare these nucleation activities, each sonicated fαS was added to un-cross-linked WT αS (Fig. 8B). Sonicated fαS of A53T and A30P/A53T displayed an almost identical time course in fluorescence that reached maximal levels at ≈4 h. In the case of E46K, the initial rates of increase in ThS signal were ≈30 FU/h, and this rate was significantly ($p<0.001$) greater than that produced by WT (≈17 FU/h), A53T (≈20 FU/h) or A30P/A53T fαS seeds (≈21 FU/h). Maximal fluorescence was observed by ≈3 h using E46K fαS seeds. On the other hand, in fαS of A30P, the initial rate of increase in ThS signal was ≈11 FU/h, and this rate was significantly smaller than that of WT, E46K, A53T or A30P/A53T fαS seeds ($p<0.001$). Maximal fluorescence was observed by ≈72 h in the fαS seeds of A30P.

Next, we examined whether cross-linked αS oligomers displayed similar nucleation activity. Adding 10% (w/w) cross-linked αS oligomers of WT eliminated the lag period and produced a quasi-hyperbolic increase in fluorescence that reached maximal levels at ≈72 h (Fig. 9A). Stable WT αS oligomers thus functioned as fibril nuclei. Nucleation activity was displayed by other mutant αS peptides, E46K, A30P, A53T and A30P/A53T oligomers as well (Fig. 9A). To compare these nucleation

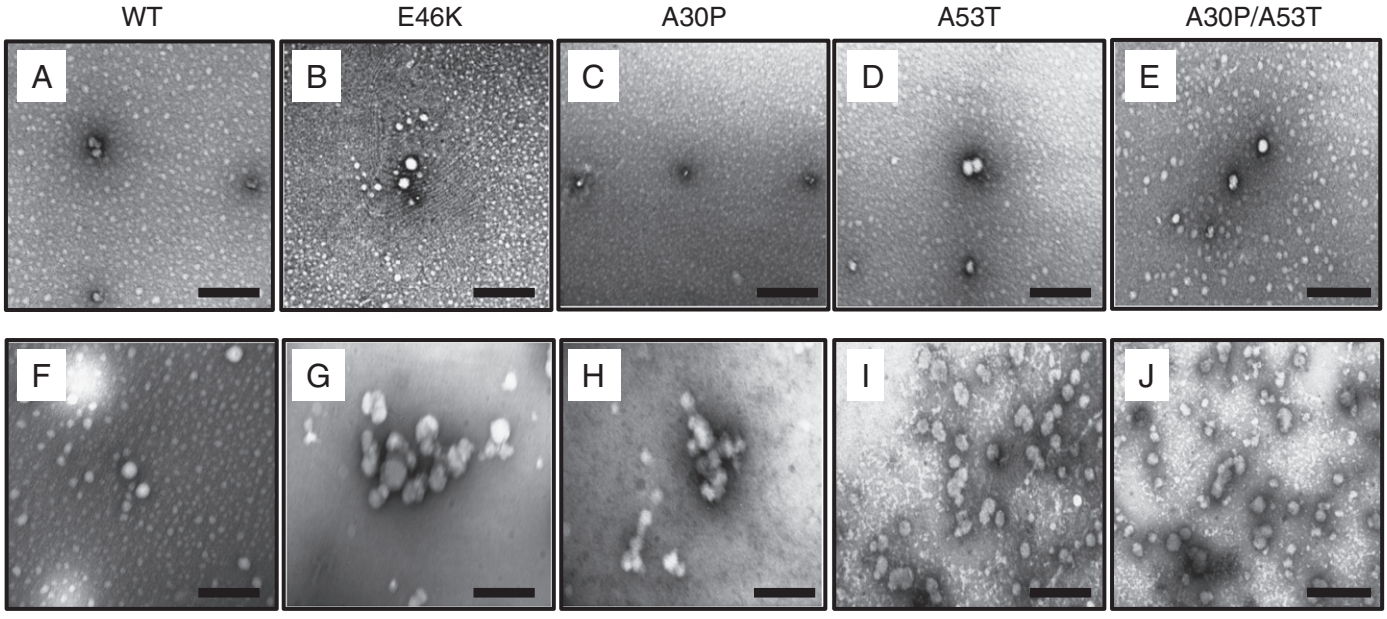

Fig. 6. EM analysis of αS oligomers. EM was performed on 70 μM un-cross-linked (A–E) and cross-linked (F–J) αS of WT (A, F), E46K (B, G), A30P (C, H), A53T (D, I) or A30P/A53T (E, J) peptide. Scale bars are 100 nm.

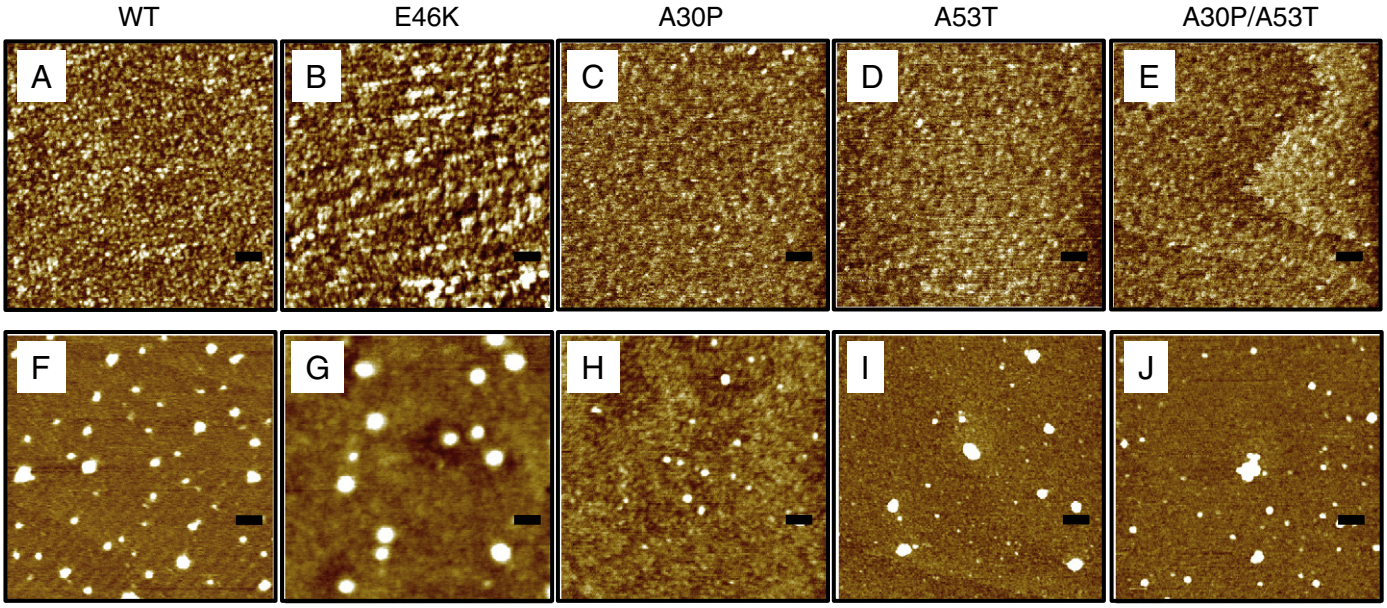

Fig. 7. AFM analysis of αS oligomers. AFM was performed on 70 μM un-cross-linked (A–E) and cross-linked (F–J) αS of WT (A, F), E46K (B, G), A30P (C, H), A53T (D, I) or A30P/A53T (E, J) peptide. Scale bars are 100 nm.

activities, each cross-linked oligomer of αS was added to un-cross-linked WT αS (Fig. 9B). Similarly to cross-linked αS oligomers of WT, cross-linked αS oligomers of A53T and A30P/A53T displayed an almost identical time course in fluorescence that reached maximal levels at ≈72 h. In the case of E46K, the initial rates of increase in ThS signal were ≈12 FU/h, and this rate was significantly ($p<0.001$) greater than that

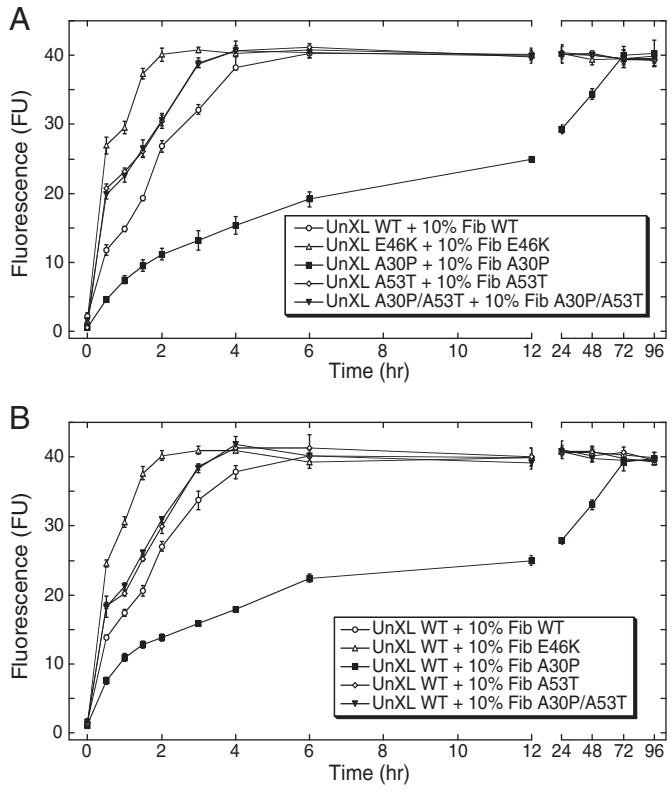

Fig. 8. Nucleation activities of sonicated αS fibrils. (A) 10% (v/v) sonicated αS fibrils (Fib) of WT (○), E46K (△), A30P (■), A53T (◇) or A30P/A53T (▼) was added to each un-cross-linked (UnXL) αS, which then was incubated for 7 d at 37 °C in 20 mM Tris buffer, pH 7.4. (B) 10% (v/v) sonicated αS fibrils (Fib) of WT (○), E46K (△), A30P (■), A53T (◇) or A30P/A53T (▼) was added to un-cross-linked (UnXL) WT αS, which then was incubated for 4 d at 37 °C in 20 mM Tris buffer, pH 7.4. Aliquots were assayed periodically using ThS. Binding is expressed as mean fluorescence (in arbitrary fluorescence units (FU)) ± S.E. Each figure comprises data obtained with 3 independent experiments.

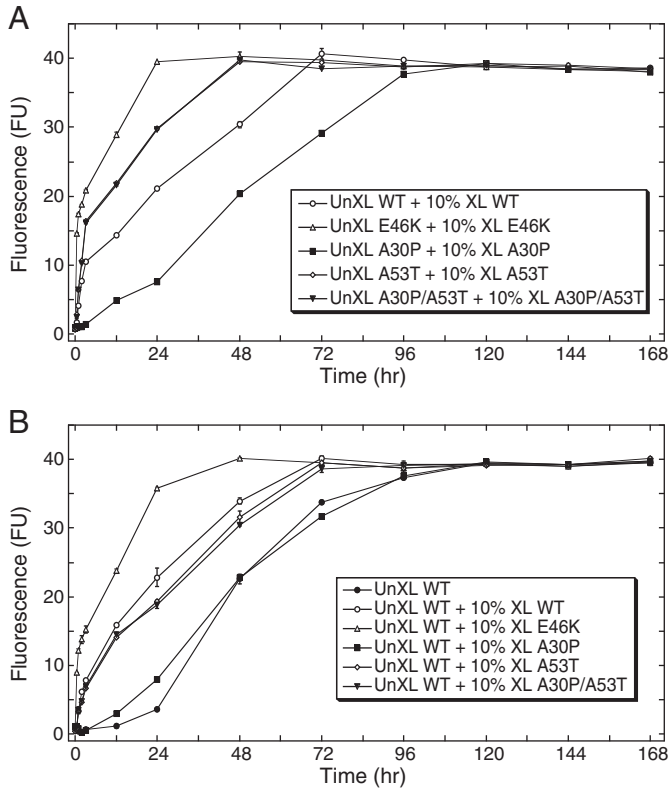

Fig. 9. Nucleation activities of αS oligomers. (A) 10% (v/v) cross-linked (XL) WT (○), E46K (△), A30P (■), A53T (◇) or A30P/A53T (▼) oligomers of αS was added to each un-cross-linked (UnXL) αS, which then was incubated for 7 d at 37 °C in 20 mM Tris buffer, pH 7.4. (B) Zero % (v/v) (●) or 10% (v/v) cross-linked (XL) WT (○), E46K (△), A30P (■), A53T (◇) or A30P/A53T (▼) oligomers of αS was added to un-cross-linked (UnXL) WT αS, which then was incubated for 7 d at 37 °C in 20 mM Tris buffer, pH 7.4. Aliquots were assayed periodically using ThS. Binding is expressed as mean fluorescence (in arbitrary fluorescence units (FU)) ± S.E. Each figure comprises data obtained in 3 independent experiments.

produced by WT, A53T or A30P/A53T αS seeds (≈3.5 FU/h). Maximal fluorescence was observed by ≈48 h using E46K αS seeds, compared to ≈72 h using WT, A53T or A30P/A53T αS seeds. On the other hand, in A30P αS, the initial rate of increase in ThS signal was ≈0.6 FU/h, and this rate was significantly smaller than that produced by WT, E46K, A53T or A30P/A53T αS seeds ($p<0.001$). Maximal fluorescence was observed by ≈120 h using A30P αS seeds.

Secondary structures of wild type and mutant αS assemblies

αS has been shown to exist predominately as a statistical coil if prepared under conditions designed to prevent its folding and self-assembly (Li et al., 2002). However, as shown above, peptide folding and assembly is a dynamic process involving an overall SC→α-helix→β-sheet transition. To determine the conformational states of the stable oligomers formed by the five peptides, CD was performed following cross-linking. Un-cross-linked αS of WT displayed spectra consistent with the SC state (Supplementary Fig. 1A). The major features of these spectra were a substantial minimum centered at≈198 nm and an inflection point at≈225 nm. In contrast, the major spectral feature displayed by the cross-linked oligomers of WT αS peptide was a population comprising mixture of α-helix and β-sheet conformers (Supplementary Fig. 1A). The spectra of un-cross-linked and cross-linked αS peptides of E46K (Supplementary Fig. 1B), A30P (Supplementary Fig. 1C), A53T (Supplementary Fig. 1D) and A30P/A53T (Supplementary Fig. 1E) were almost same as those of the wild type αS peptide.

Discussion

The etiology of LBD is complex, but the aggregation of αS has been suggested to be a seminal pathogenetic agent (Brown, 2010; Ono et al., 2008; Uversky, 2007). Three missense mutations in the αS gene have been identified in familial cases of early onset PD or LBD: the A53T mutation in a large Italian-American family with PD, known as the Contursi kindred (Polymeropoulos et al., 1997); the A30P mutation in a German family with PD (Kruger et al., 1998); and the E46K mutation in a Spanish family with LBD characterized by autosomal dominant parkinsonism, dementia, and visual hallucinations of variable severity (Zarranz et al., 2004). These findings suggest that a single mutation in the human αS gene is sufficient to result in the LBD phenotype (Uversky, 2007). By studying these mutations we may find out some clues of the biophysical basis for disease causation. We found, relative to peptides containing the WT αS N terminal sequence, that E46K mutations facilitated fαS formation as well as secondary transition, oligomerization, and produced larger oligomeric assemblies, whereas A30P mutations decreased them. Stable oligomers of E46K αS were more potent nucleators of higher-order assembly than were WT oligomers, whereas those of A30P αS were weaker nucleators of higher-order assembly.

First, we examined how E46K, A30P, A53T or A30P/A53T influenced fαS formation using ThS binding and EM assays in vitro. We found that E46K, A53T and A30P/A53T αS accelerated the formation of fαS, especially the elongation process compared with WT, whereas A30P αS decelerated the formation of fαS, especially the elongation process. The overall activity of fαS formation was in the order of: E46K>A53T=A30P/A53T>WT>A30P. All mutations have been reported to influence the propensity of fαS formation, but the results are not necessarily consistent. Narhi et al. (1999) reported accelerated fαS formation for all A30P, A53T and A30P/A53T mutants; A30P αS formed fαS slightly faster than WT αS, and both A53T and A30P/A53T αS formed much faster. Conway et al. (1998, 2000b) reported that the A53T mutation increased the propensity of fαS formation, but the A30P mutation did not. There are a few reports that the A30P mutation decreased fαS formation, especially the nucleation phase (Conway et al., 2000b; Yonetani et al., 2009). The E46K mutation has been reported to increase the propensity of fαS formation, but this effect was less pronounced than that of the A53T mutation (Greenbaum et al., 2005). This discrepancy may be due to the difference of sample preparation such as buffer, pH and αS concentration.

Second, we studied the conformational dynamics of the αS systems. Examination of temporal changes in secondary structure revealed that E46K, A53T and A30P/A53T mutations accelerated the rate of the SC→α-helix→β-sheet transition; the change of E46K αS was much faster than that of WT αS, and those of both A53T and A30P/A53T αS were slightly faster. Especially, the acceleration of E46K αS was ~2.5-fold as determined by the $t_{1/2}$ for the transition, and the maximal observed transition rate from SC to ordered secondary structures of E46K αS was biggest among the five different αS peptides. The change of A30P αS was slightly slower than that of WT αS. These results were compatible with the results of fαS formation, and suggest that the αS mutations cause substantial changes in peptide structural order that influence monomer folding and are necessary for higher-order assembly, including oligomerization and fibril nucleation and elongation.

Third, we focused primarily on the oligomerization process, which is hypothesized to be the most important process in LBD pathobiology (Danzer et al., 2007; Karpinar et al., 2009; Outeiro et al., 2008; Wright et al., 2009). The E46K αS produced an oligomer distribution in which the highest observed oligomer order exceeded that of the WT αS. By contrast, the A30P αS produced an oligomer distribution with a lower oligomer order than the WT αS. The oligomer size frequency distribution is controlled by the proximity, chemical reactivity, and chemical accessibility of amino acid side-chains, predominantly the phenol group of Tyr (Bitan and Teplow, 2004; Fancy and Kodadek, 1999; Fancy et al., 2000). The change in order was accompanied by a change in size, as determined by AFM (z-axis value) analyses. Cross-linked oligomers of WT and mutant αS were smaller than those reported by other groups (Giehm et al., 2011; Kim et al., 2009). In our study, E46K αS produced an assembly with larger oligomers than WT αS, whereas A30P αS produced an assembly with smaller oligomers. These data were consistent with our determination of oligomer size frequency distribution, which showed skewing toward higher or lower order with the mutant peptides. We recently reported that a direct correlation between oligomer order and size, that is, that higher-n order oligomers have larger particles in the Aβ system (Ono et al., 2009, 2010). The stabilized oligomers in each system showed a consistent rank order of size, E46K>A53T=A30P/A53T=WT>A30P. Although dynamic light scattering studies showed faster oligomerization in A30P and A53T αS than in WT αS (Karpinar et al., 2009), a detailed biochemical analysis has not been reported.

Since the effect of the mutation on the αS assembly process should help to understand the disease mechanism(s) of LBD, we examined the relative ability of fαS as well as stabilized oligomers to nucleate the assembly of ThS-positive structures. We found that αS exhibited a substantial lag period (≈0.5 d) that was eliminated by addition of WT and mutant oligomers although this nucleation activity of each αS oligomer was smaller than that of each fαS. The rank order of the rates of propagation of ThS-positive structure (dFU/dt) was E46K>A53T=A30P/A53T=WT>A30P. These mutations facilitate the structural organization of αS, and the structure(s) thus formed are potent nucleators of the assembly of the ThS-positive αS structure.

What type of structural effects might be caused by these αS mutations? Two classes of effects exist, local and global. By definition, the local effects include alteration in peptide chain structure at or immediately adjacent to the sites of the amino acid substitutions. It is not clear whether local folding motifs may be affected. What is clear is that the oligomerization process is affected. Again, by definition, this means that intermolecular interactions must be altered. We can speculate three mechanisms of the alteration: (1) the same monomer folding necessary for oligomerization as that of WT αS peptide influences occurrence frequency of other mutated αS oligomerization and the same residues mediating the intermolecular interactions with

the WT αS peptide are involved in other mutated αS (but do not include Pro[30], Lys[46], or Thr[53]); (2) intermolecular interactions involving Lys[46] or Thr[53] are more stable than those involving Glu[46] or Ala[53], whereas the interactions involving Pro[30] are less stable than those involving Ala[30]; and (3) a different monomer folding that influences a propensity for self-association but which may or may not require direct intermolecular interactions involving Pro[30], Lys[46], or Thr[53] occurs.

Structurally, αS in its free state shows a weak propensity for a helical structure throughout the N-terminal lipid-binding domain and a preference for more extended conformations in the acidic C-terminal region (Eliezer et al., 2001). Intramolecular contacts between the acidic C-terminal tail of αS and its N-terminal region have been proposed to regulate αS assembly, A30P and A53T mutations have been reported to lead to a local decrease in the helical propensity of the protein—an effect that has been proposed to facilitate the assembly of these two mutants into the β-sheet-rich conformers (Bussell and Eliezer, 2001). The presence of an amphipathic helical structure, combined with the known role of the hydrophic NAC region of αS in mediating intermolecular interactions, also led to the hypothesis that transient long-range intramolecular contacts could protect αS from self-assembly (Bussell and Eliezer, 2001). NMR studies confirmed the presence of long-range contacts in αS, but they were observed predominantly between the acidic C-terminal tail and both the NAC region and a region near the N-terminus of the protein (Bertoncini et al., 2005b; Dedmon et al., 2005). Although a subsequent report indicated that the A30P and A53T mutations disrupt these long-range interactions, and this effect was also proposed to underlie the ability of these mutations to facilitate αS assembly in vitro (Bertoncini et al., 2005a), different effects on intramolecular interactions have not been reported. Surprisingly, Rospigliosi et al. (2009) reported that the E46K mutation did not interfere with C-terminal-to-N-terminal contacts but rather enhanced such contacts, and that A30P and A53T mutations reduced such contacts. They suggested that C-terminal-to-N-terminal contacts in αS did not strongly influence self-assembly, and that the dominant mechanism by which these PD-linked mutations facilitate αS assembly may be altering the physicochemical properties of the protein such as net charge (E46K) and secondary structure propensity (A30P and A53T) (Rospigliosi et al., 2009). Further mechanistic studies focused on αS N terminal structural dynamics are needed.

A clear difference in onset age or clinical course between mutations has not been reported. Dementia was common in families with both A53T and E46K mutations (Kruger et al., 1998; Polymeropoulos et al., 1997; Zarranz et al., 2004), but uncommon in a family with the A30P mutation (Kruger et al., 1998; Polymeropoulos et al., 1997; Zarranz et al., 2004). The levodopa-response was good in a family with A30P or A53T mutation, but was limited in the early stage of the disease in a family with LBD with E46K mutation (Zarranz et al., 2004). The patients in a family with E46K mutation had a cognitive deficit in the early stage of disease and DLB pathology; a high density of LBs was present not only in the subcortical nuclei but also in the parahippocampus, amygdala and cortex (Zarranz et al., 2004). The patients in families with the A30P or A53T mutation also exhibited diffuse LBs pathology (Markopoulou et al., 2008; Seidel et al., 2010). Although the widespread distribution of LBs formation in LBD with the E46K mutation (Zarranz et al., 2004) may be related to accelerated assembly of E46K αS observed in our study, it is difficult to correlate our in vitro results to clinicopathological findings reported in patients with these mutations. Other proteins such as transcriptional cofactor high mobility group protein 1, brain-specific protein p25 α tublin, and aglin have been identified as components of LBs (Alim et al., 2002; Lindersson et al., 2004, 2005; Liu et al., 2005). A difference in the interaction of αS with these proteins may be responsible for the difference in αS aggregation and LBs formation among WT and mutant αS peptides.

In conclusion, E46K αS accelerated the kinetics of the secondary structure change and oligomerization, whereas A30P αS decelerated them. These effects were reflected in changes in average oligomer size and activities as nucleators of the self-assembly process. The mutant oligomers of E46K αS functioned as fibril seeds significantly more efficiently than those of WT αS, while the mutant oligomers of A30P αS were less efficient. Our results that familial mutations had opposite effects at early stages of αS assembly may provide new insight into the molecular mechanism of LBD.

Supplementary materials related to this article can be found online at doi:10.1016/j.nbd.2011.05.025.

Acknowledgments

We acknowledge the support of a grant from the Knowledge Cluster Initiative [High-Tech Sensing and Knowledge Handling Technology (Brain Technology)] (M.Y.), a grant to the Amyloidosis Research Committee from the Ministry of Health, Labor, and Welfare, Japan (M.Y. and K.O.), Alumni Association of the Department of Medicine at Showa University (K.O.), Kanae Foundation for the Promotion of Medical Science (K.O.), and Nagao Memorial fund (K.O.). The authors declare no conflicts of interest.

References

Alim, M.A., et al., 2002. Tubulin seeds α-synuclein fibril formation. J. Biol. Chem. 277, 2112–2117.
Baba, M., et al., 1998. Aggregation of α-synuclein in Lewy bodies of sporadic Parkinson's disease and dementia with Lewy bodies. Am. J. Pathol. 152, 879–884.
Bertoncini, C.W., et al., 2005a. Familial mutants of α-synuclein with increased neurotoxicity have a destabilized conformation. J. Biol. Chem. 280, 30649–30652.
Bertoncini, C.W., et al., 2005b. Release of long-range tertiary interactions potentiates aggregation of natively unstructured α-synuclein. Proc. Natl. Acad. Sci. U. S. A. 102, 1430–1435.
Bitan, G., Teplow, D.B., 2004. Rapid photochemical cross-linking—a new tool for studies of metastable, amyloidogenic protein assemblies. Acc. Chem. Res. 37, 357–364.
Bitan, G., et al., 2001. Amyloid β-protein oligomerization: prenucleation interactions revealed by photo-induced cross-linking of unmodified proteins. J. Biol. Chem. 276, 35176–35184.
Brown, D.R., 2010. Oligomeric α-synuclein and its role in neuronal death. IUBMB Life 62, 334–339.
Bussell Jr., R., Eliezer, D., 2001. Residual structure and dynamics in Parkinson's disease-associated mutants of α-synuclein. J. Biol. Chem. 276, 45996–46003.
Chartier-Harlin, M.C., et al., 2004. α-Synuclein locus duplication as a cause of familial Parkinson's disease. Lancet 364, 1167–1169.
Conway, K.A., et al., 1998. Accelerated in vitro fibril formation by a mutant α-synuclein linked to early-onset Parkinson disease. Nat. Med. 4, 1318–1320.
Conway, K.A., et al., 2000a. Fibrils formed in vitro from α-synuclein and two mutant forms linked to Parkinson's disease are typical amyloid. Biochemistry 39, 2552–2563.
Conway, K.A., et al., 2000b. Acceleration of oligomerization, not fibrillization, is a shared property of both α-synuclein mutations linked to early-onset Parkinson's disease: implications for pathogenesis and therapy. Proc. Natl. Acad. Sci. U. S. A. 97, 571–576.
Danzer, K.M., et al., 2007. Different species of α-synuclein oligomers induce calcium influx and seeding. J. Neurosci. 27, 9220–9232.
Davidson, W.S., et al., 1998. Stabilization of α-synuclein secondary structure upon binding to synthetic membranes. J. Biol. Chem. 273, 9443–9449.
Dedmon, M.M., et al., 2005. Heat shock protein 70 inhibits α-synuclein fibril formation via preferential binding to prefibrillar species. J. Biol. Chem. 280, 14733–14740.
Duda, J.E., et al., 2000. Neuropathology of synuclein aggregates. J. Neurosci. Res. 61, 121–127.
Eliezer, D., et al., 2001. Conformational properties of α-synuclein in its free and lipid-associated states. J. Mol. Biol. 307, 1061–1073.
Evans, K.C., et al., 1995. Apolipoprotein E is a kinetic but not a thermodynamic inhibitor of amyloid formation: implications for the pathogenesis and treatment of Alzheimer disease. Proc. Natl. Acad. Sci. U. S. A. 92, 763–767.
Fancy, D.A., Kodadek, T., 1999. Chemistry for the analysis of protein–protein interactions: rapid and efficient cross-linking triggered by long wavelength light. Proc. Natl. Acad. Sci. U. S. A. 96, 6020–6024.
Fancy, D.A., et al., 2000. Scope, limitations and mechanistic aspects of the photo-induced cross-linking of proteins by water-soluble metal complexes. Chem. Biol. 7, 697–708.
Farrer, M., et al., 2004. Comparison of kindreds with parkinsonism and α-synuclein genomic multiplications. Ann. Neurol. 55, 174–179.
Fredenburg, R.A., et al., 2007. The impact of the E46K mutation on the properties of α-synuclein in its monomeric and oligomeric states. Biochemistry 46, 7107–7118.
Fuchs, J., et al., 2007. Phenotypic variation in a large Swedish pedigree due to SNCA duplication and triplication. Neurology 68, 916–922.

Fujiwara, H., et al., 2002. α-Synuclein is phosphorylated in synucleinopathy lesions. Nat. Cell Biol. 4, 160–164.
Giasson, B.I., et al., 1999. Mutant and wild type human α-synucleins assemble into elongated filaments with distinct morphologies in vitro. J. Biol. Chem. 274, 7619–7622.
Giehm, L., et al., 2011. Low-resolution structure of a vesicle disrupting α-synuclein oligomer that accumulates during fibrillation. Proc. Natl. Acad. Sci. U. S. A. 108, 3246–3251.
Goldberg, M.S., Lansbury Jr., P.T., 2000. Is there a cause-and-effect relationship between α-synuclein fibrillization and Parkinson's disease? Nat. Cell Biol. 2, E115–E119.
Greenbaum, E.A., et al., 2005. The E46K mutation in α-synuclein increases amyloid fibril formation. J. Biol. Chem. 280, 7800–7807.
Groenning, M., 2009. Binding mode of Thioflavin T and other molecular probes in the context of amyloid fibrils-current status. J. Chem. Biol. 3, 1–18.
Ibanez, P., et al., 2004. Causal relation between α-synuclein gene duplication and familial Parkinson's disease. Lancet 364, 1169–1171.
Karpinar, D.P., et al., 2009. Pre-fibrillar α-synuclein variants with impaired β-structure increase neurotoxicity in Parkinson's disease models. EMBO J. 28, 3256–3268.
Kim, H.Y., et al., 2009. Structural properties of pore-forming oligomers of α-synuclein. J. Am. Chem. Soc. 131, 17482–17489.
Kruger, R., et al., 1998. Ala30Pro mutation in the gene encoding α-synuclein in Parkinson's disease. Nat. Genet. 18, 106–108.
LeVine III, H., 1993. Thioflavine T interaction with synthetic Alzheimer's disease β-amyloid peptides: detection of amyloid aggregation in solution. Protein Sci. 2, 404–410.
LeVine III, H., 1999. Quantification of β-sheet amyloid fibril structures with thioflavin T. Methods Enzymol. 309, 274–284.
Li, J., et al., 2002. Conformational behavior of human α-synuclein is modulated by familial Parkinson's disease point mutations A30P and A53T. Neurotoxicology 23, 553–567.
Lindersson, E.K., et al., 2004. α-Synuclein filaments bind the transcriptional regulator HMGB-1. Neuroreport 15, 2735–2739.
Lindersson, E., et al., 2005. p25α stimulates α-synuclein aggregation and is co-localized with aggregated α-synuclein in α-synucleinopathies. J. Biol. Chem. 280, 5703–5715.
Liu, I.H., et al., 2005. Agrin binds α-synuclein and modulates α-synuclein fibrillation. Glycobiology 15, 1320–1331.
Markopoulou, K., et al., 2008. Clinical, neuropathological and genotypic variability in SNCA A53T familial Parkinson's disease. Variability in familial Parkinson's disease. Acta Neuropathol. 116, 25–35.
Naiki, H., Nakakuki, K., 1996. First-order kinetic model of Alzheimer's β-amyloid fibril extension in vitro. Lab. Invest. 74, 374–383.
Narhi, L., et al., 1999. Both familial Parkinson's disease mutations accelerate α-synuclein aggregation. J. Biol. Chem. 274, 9843–9846.
Nishie, M., et al., 2004. Accumulation of phosphorylated α-synuclein in the brain and peripheral ganglia of patients with multiple system atrophy. Acta Neuropathol. 107, 292–298.
Nishioka, K., et al., 2006. Clinical heterogeneity of α-synuclein gene duplication in Parkinson's disease. Ann. Neurol. 59, 298–309.
Okochi, M., et al., 2000. Constitutive phosphorylation of the Parkinson's disease associated α-synuclein. J. Biol. Chem. 275, 390–397.
Ono, K., Yamada, M., 2006. Antioxidant compounds have potent anti-fibrillogenic and fibril-destabilizing effects for α-synuclein fibrils in vitro. J. Neurochem. 97, 105–115.
Ono, K., et al., 2008. α-Synuclein assembly as a therapeutic target of Parkinson's disease and related disorders. Curr. Pharm. Des. 14, 3247–3266.
Ono, K., et al., 2009. Structure-neurotoxicity relationships of amyloid β-protein oligomers. Proc. Natl. Acad. Sci. U. S. A. 106, 14745–14750.
Ono, K., et al., 2010. Effects of the English (H6R) and Tottori (D7N) familial Alzheimer disease mutations on amyloid β-protein assembly and toxicity. J. Biol. Chem. 285, 23186–23197.
Outeiro, T.F., et al., 2008. Formation of toxic oligomeric α-synuclein species in living cells. PLoS One 3, e1867.
Polymeropoulos, M.H., et al., 1997. Mutation in the α-synuclein gene identified in families with Parkinson's disease. Science 276, 2045–2047.
Pronin, A.N., et al., 2000. Synucleins are a novel class of substrates for G protein-coupled receptor kinases. J. Biol. Chem. 275, 26515–26522.
Rospigliosi, C.C., et al., 2009. E46K Parkinson's-linked mutation enhances C-terminal-to-N-terminal contacts in α-synuclein. J. Mol. Biol. 388, 1022–1032.
Seidel, K., et al., 2010. First appraisal of brain pathology owing to A30P mutant α-synuclein. Ann. Neurol. 67, 684–689.
Singleton, A.B., et al., 2003. α-Synuclein locus triplication causes Parkinson's disease. Science 302, 841.
Spillantini, M.G., et al., 1998. α-Synuclein in filamentous inclusions of Lewy bodies from Parkinson's disease and dementia with Lewy bodies. Proc. Natl. Acad. Sci. U. S. A. 95, 6469–6473.
Uversky, V.N., 2007. Neuropathology, biochemistry, and biophysics of α-synuclein aggregation. J. Neurochem. 103, 17–37.
Uversky, V.N., et al., 2001. Evidence for a partially folded intermediate in α-synuclein fibril formation. J. Biol. Chem. 276, 10737–10744.
Volles, M.J., Lansbury Jr., P.T., 2002. Vesicle permeabilization by protofibrillar α-synuclein is sensitive to Parkinson's disease-linked mutations and occurs by a pore-like mechanism. Biochemistry 41, 4595–4602.
Wood, S.J., et al., 1999. α-Synuclein fibrillogenesis is nucleation-dependent. Implications for the pathogenesis of Parkinson's disease. J. Biol. Chem. 274, 19509–19512.
Wright, J.A., et al., 2009. Unique copper-induced oligomers mediate α-synuclein toxicity. FASEB J. 23, 2384–2393.
Yonetani, M., et al., 2009. Conversion of wild-type α-synuclein into mutant-type fibrils and its propagation in the presence of A30P mutant. J. Biol. Chem. 284, 7940–7950.
Zarranz, J.J., et al., 2004. The new mutation, E46K, of α-synuclein causes Parkinson and Lewy body dementia. Ann. Neurol. 55, 164–173.